DETERMINATION OF 3-D VELOCITY FIELD FROM THE FOUR HOT-WIRE OUTPUT SIGNALS USING *THREE AGAINST ONE* ALGORITHM

by

Milovan KOTUR[a], Pero PETROVIĆ[a], and Viktor ŠAJN[b]*

[a] Faculty of Mechanical Engineering, University of Banja Luka, Banja Luka, Republic of Srpska, Bosnia & Herzegovina
[b] Faculty of Mechanical Engineering, University of Ljubljana, Ljubljana, Slovenia

Original scientific paper
https://doi.org/10.2298/TSCI170630237K

The advantage of "three against one" algorithm for determination of 3-D velocity field from the four hot-wires output signals is presented. Three tests of this algorithm, with differently defined dependence between velocity components and probe output signals are conducted. Test with generalized hot-wire cooling law shows better results in comparison to the test based on King-Jorgensen equations. It is shown that "three against one" algorithm has some advantage near the border of uniqueness range in comparison to the existing algorithms.

Key words: *four sensors hot-wire probe, "three against one" algorithm, King-Jorgensen cooling law, generalized hot-wire cooling law*

Introduction

Hot-wire anemometers (HWA) are intensively used to measure velocity vector components and temperature fluctuation in turbulent flows. They provide measurements in a wide fluid velocity range, with high accuracy and frequency response. Operation of a HWA is based on the dependence of sensor electrical resistance on temperature. In a flow field, hot-wire detects heat transfer from a heated sensors to its environment. The voltage output of a HWA is a non-linear function of fluid velocity components.

The dependence between output voltage and fluid velocity vector, $\vec{V}_R$, of the constant temperature HWA (CTA) according to King's law is:

$$E^2 = A + B\vec{V}_N^{\,p} \tag{1}$$

where $\vec{V}_N$ is the velocity component perpendicular to the sensor longitudinal axis, fig. 1. The precise values of constants A and B should be determined experimentally. The constant p is dependent on the mechanism of forced convection flow and its value is between 0.35 and 0.5 [1].

Generally, when the orientation of velocity vector is optional, the influence of all three velocity components should be taken into account by replacing the normal component of fluid velocity vector $\vec{V}_N$, by so-called *effective cooling velocity* V_{eff}.

One definition of effective cooling velocity of the hot-wire, was suggested by Jorgensen [1]:

* Corresponding author, e-mail: viktor.sajn@fs.uni-lj.si

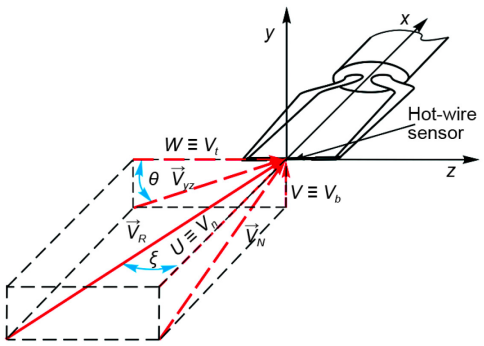

Figure 1. Components (*U, V, W*) of an arbitrary oriented fluid velocity vector, $\vec{V}_R$, on the hot-wire with normal sensor

$$V_{\text{eff}}^2 = V_{\text{n}}^2 + kV_{\text{t}}^2 + hV_{\text{b}}^2 \tag{2}$$

where V_{n} is the velocity component normal to the sensor, in the plane of the sensor and its supporting prongs (yaw plane), V_{t} – the velocity component tangential to the sensor, and V_{b} – a binormal velocity component in the plane perpendicular to the sensor and its supporting prongs (pitch plane, fig. 1). Coefficients k and h are determined experimentally. The U velocity component is also known as longitudinal and V_{vz} as span wise velocity component.

Willmarth [2] and Dobbeling *et al.* [3] presented an illustrative graphical analysis of the hot-wire response equation. For an ideal hot-wire with an infinite long hot-wire sensor (k = 0, h = 1), Willmarth [2] showed that infinite number of possible fluid velocity vectors of various intensity and directions give the same response. Their tips are at the centre of the sensor and their tails lay on a cylinder of infinite length. In the case of hot-wire with two sensors inclined at 45°, an infinite number of possible fluid velocity vectors which give the same response are defined with intersection of the surfaces of two orthogonal cylinders. In the case of hot-wire with three orthogonal sensors, intersection of the surfaces of three orthogonal cylinders can occur at up to eight points *i. e.* eight velocity vectors that can produce a single set of three different signals.

A more realistic approach in the interpreting of multiple hot-wires signals based on Jorgensen effective cooling velocity, eq. (2), was conducted by Dobbeling *et al.* [3]. Probe behaviour is graphically represented by an affine contraction of a rotational ellipsoid. Similar conclusion related to the number of possible solutions can be obtained as presented in [2]. For "X" wire probes, there is an infinite number of solutions for the instantaneous fluid velocity vector. For three wire probes, commonly constructed with three orthogonal wires, in general up to eight different solutions exist, produce by a single set of three sensor signals.

Generally, for any number of sensors included in a hot-wire probe, multiple solutions of the sensor response results can be obtained. These solutions define different velocity vectors for any specific set of anemometer output signals. This is known as *uniqueness* problem. During the last forty years, this problem was analysed by many researchers, and the results of new studies are presented in [4, 5].

Previous research showed that there exist a solution domain, known as uniqueness domain, where the velocity vector can be uniquely determined. The border of this domain depends on the orientation and number of hot-wire sensors. Schematic view of uniqueness domain, is shown in fig. 2. It is assigned by a dot line and bounded by the value of angle, ξ, that corre-

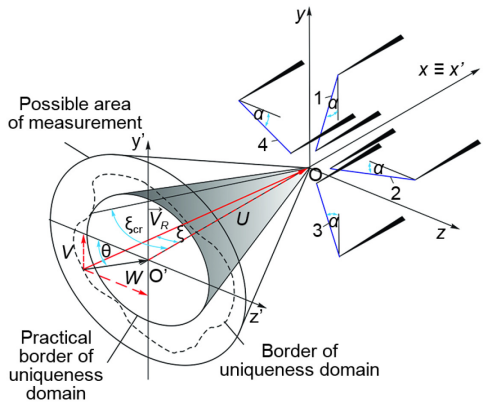

Figure 2. Schematic view of uniqueness domain, for multi-sensor hot-wire probe, in Cartesian and spherical co-ordinates

sponds to this line. The practical border of the uniqueness domain, where the solution is always unique for any value of angle θ, is determined by the minimum or critical value of angle ξ, $\xi = \xi_{cr}$.

Starting from eq. (2), Vukoslavčević *et al.* [4], showed that the practical border of the uniqueness domain, in the case of hot-wire probe with four sensors, can be defined:

$$\xi_{cr} = \pm \arctan \sqrt{\frac{2(\cos^2 \alpha + k \sin^2 \alpha)}{\sin^2 \alpha + k \cos^2 \alpha + h}} \tag{3}$$

In the case of a four-sensor ideal probe, for which we can adopt $k = 0$, $h = 1$ and sensor angle $\alpha = 34°$, this equation give the value of critical angles of $\xi_{cr} = 45.66°$.

Processing of experimental data of a four sensor hot-wire probe with sensor inclination angle of 34° are presented in this paper. In order to determine the velocity components from the four output signals a numerical algorithm known as *three against one* is used. Numerical test of this algorithm for virtual ideal hot-wire probe with four sensors, based on different definitions of effective cooling velocity (cosines law, Hinze equation, and Jorgensen equation) of the hot-wire is presented in [6-8].

Three tests of the algorithm are conducted, with two differently defined cooling laws (dependence between velocity and output signals), in order to find out which of them gives better results using real experimental data.

First test was based on King-Jorgensen cooling law eqs. (1) and (2). The fluid velocity components, V_n, V_t, and V_b in fig. 1, and the Cartesian components, U, V, and W, in the case of sensors inclined under angle, α fig. 2, are related by the following expressions:

$$\begin{aligned} V_{\text{eff}\,1,3}^2 &= (U \cos\alpha \mp V \sin\alpha)^2 + k_{1,3}(U \sin\alpha \pm V \cos\alpha)^2 + h_{1,3} W^2 \\ V_{\text{eff}\,2,4}^2 &= (U \cos\alpha \mp W \sin\alpha)^2 + k_{2,4}(U \cos\alpha \pm W \sin\alpha)^2 + h_{2,4} V^2 \end{aligned} \tag{4}$$

In the second test, the algorithm was based on so-called *generalised law of hot-wire cooling* [1]. Starting from the empirical law of Jorgensen, eq. (2), effective cooling velocity for the sensor i can be defined in the form:

$$V_{\text{eff}_i}^2 = c_{i1} U^2 + c_{i2} V^2 + c_{i3} W^2 + c_{i4} UV + c_{i5} UW + c_{i6} VW \tag{5}$$

where calibration coefficients c_{ij} (i = 1-4, j = 1-6) lumped together the influence of thermal contamination and geometrical imperfections. Dividing by c_{ij} this expression can be rearranged in the following form:

$$V_{\text{eff}\,g_i}^2 = U^2 + a_{i1} V^2 + a_{i2} W^2 + a_{i3} UV + a_{i4} UW + a_{i5} VW \tag{6}$$

The relation between the effective cooling velocity (6) and anemometer voltage outputs can be established by a fourth order polynomial fit:

$$V_{\text{eff}\,g_i}^2 = \sum_{k=1}^{5} b_{ik} E_i^{j-1} \tag{7}$$

where constants a_{ik} and b_{ik} (i = 1-4, k = 1-5), should be determined in least square fit calibration procedures.

In the third test, the *three against one* algorithm based on *generalised law of hot-wire cooling* is compared to the one of the best known approach described in [1] (which is also based on *generalised law of hot-wire cooling*), using real experimental data for two ranges of angle ξ.

Short description of the *three against one* algorithm

Detailed description of the *three against one* algorithm is given in [6-8]. In order to experimentally test it, this algorithm was a little modified. The position of fluid velocity vector, $\vec{V}_R$, is defined with two angles ξ and θ (figs. 1 and 2).

The *three against one* algorithm, based on differently defined dependence between *effective cooling velocity* V_{eff} and output voltage, presented in [6-8], was originally composed of two subroutines. The first one [8], based on the eqs. (2), and (1) calculates corresponding set of output voltages for each sensor ($E_1 - E_4$). The second subroutine has a task to unambiguously define the fluid velocity vector from the set of output voltages obtained from the first subroutine (reverse mapping).

A set of four output voltages from a four sensors hot-wire can be obtained experimentally for various pitch, yaw and combined pitch/yaw angles. From that reason we test only second subroutine of the *three against one* algorithm.

As presented in [6-8], the second subroutine of the *three against one* algorithm could have most two separated iterative cycles. Generally, both iterative cycles have the same basic elements which were shown in fig. 3. Based on eq. (1) (in the case of test King-Jorgensen) or on eq. (7) (in the case of *generalized law of hot-wire cooling*), and experimentally determined coefficients *A, B* (in the case of test King-Jorgensen), and b_{ik} (in the case of *generalized hot-wire cooling law*), second subroutine, first calculates effective cooling velocities at each of the four sensors. Then, based on the intensity of the these four effective cooling

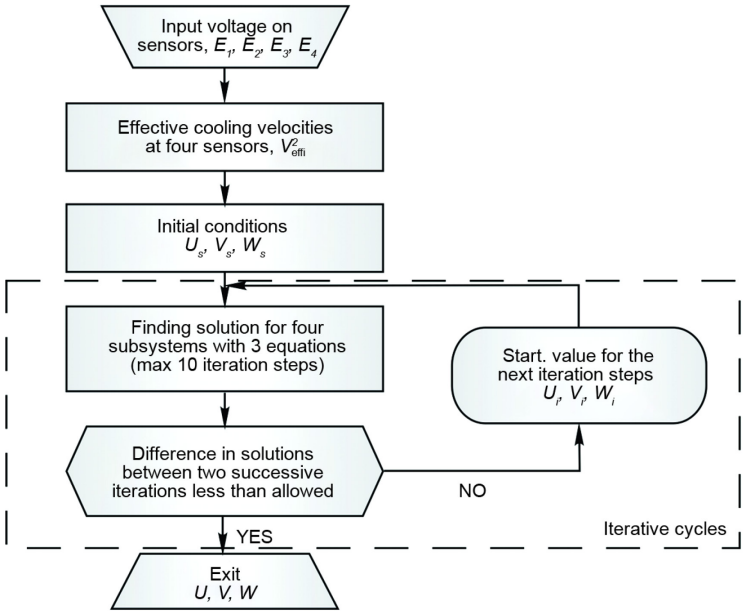

Figure 3. Basic elements of the *three against one* algorithm

velocities, V_{eff}^2, (i = 1-4), second subroutine should unambiguously define components *U, V,* and *W* of the velocity vector, $\vec{V}_R$ (fig. 2) by using the system of eq. (2) or eq. (6) which can be presented in general form:

$$\begin{aligned} Eq_1: &\quad V_{\text{eff}\,1}^2 = f_1(U,V,W) \\ Eq_2: &\quad V_{\text{eff}\,2}^2 = f_2(U,V,W) \\ Eq_3: &\quad V_{\text{eff}\,3}^2 = f_3(U,V,W) \\ Eq_4: &\quad V_{\text{eff}\,4}^2 = f_4(U,V,W) \end{aligned} \tag{8}$$

The system of eq. (8) is non-linear and has several solutions, of which only one is physically correct or, in other word, exists in the flow field. As we have three unknown parameters (components of intensity *U, V,* and *W*), from the system of eq. (8), we can create four different subsystems with three non-linear equations:

$$S1 = \begin{cases} Eq_2 \\ Eq_3 \\ Eq_4 \end{cases} \quad S2 = \begin{cases} Eq_1 \\ Eq_3 \\ Eq_4 \end{cases} \quad S3 = \begin{cases} Eq_1 \\ Eq_2 \\ Eq_4 \end{cases} \quad S4 = \begin{cases} Eq_1 \\ Eq_2 \\ Eq_3 \end{cases} \tag{9}$$

Each subsystem of non-linear eq. (9) is linearly independent from the others. In order to find a solution for each of the four subsystems of non-linear equations we use Newton's iterative methods. Theoretically, physically correct solution *i. e.* components of velocity vectors of four subsystems eq. (9), should be the same:

$$\begin{aligned} U &= U_1 = U_2 = U_3 = U_4 \\ V &= V_1 = V_2 = V_3 = V_4 \\ W &= W_1 = W_2 = W_3 = W_4 \end{aligned} \tag{10}$$

where indices 1, 2, 3, and 4 marks calculated components of fluid velocity vectors obtained from the four subsystems, eq. (9).

The *three against on*e algorithm calculates starting values for the next iteration step, on the assumption that solution which most deviates from the mean value of the four obtained solutions in present step of iteration is discarded as physically inadequate. The mean value of solutions in each step of iteration *l* is defined by the following equations:

$$\bar{U}_{ml} = \frac{1}{4}\sum_{r=1}^{4} U_{r,l}, \qquad \bar{V}_{ml} = \frac{1}{4}\sum_{r=1}^{4} V_{r,l}, \qquad \bar{W}_{ml} = \frac{1}{4}\sum_{r=1}^{4} W_{r,l} \tag{11}$$

where indexes *r* (*r* = 1-4) represents solution of corresponding subsystem of eq. (9), (calculated value of *U, V,* and *W*) in the *l* (*l* = 1-10), step of iterations. The starting values for the next iteration step, are determined as the average value of the remaining three solutions of systems of eq. (9). The procedure is to be repeated until the difference between the starting values and the obtained solution, in present step of iteration, becomes less than allowed or after defined number of iterations. If after defined number of iterations (in this test, max number of iterations was limited on ten), difference between the starting values and the solutions does not become less then allowed, the last iteration is accepted as physical solution.

Testing the *three against one* algorithm using experimental data

In order to minimize the influence of thermal contamination and flow blockade effects and focus the study on the *three against one* algorithm, a two sensor V-shaped probe, whose sketch is shown in fig. 4(a), and photo in fig. 4(b) is used.

The sensors are assigned in accordance with the assignment given in fig. 2. The response of sensors 1 and 3 is obtained by rotating the probe for 90° and repeating the pitch and yaw variation. This approach is possible in the probe calibration procedure only, because the probe is calibrated in uniform steady-flow. The advantage of this approach is that the thermal and flow blockade influence of sensor 1 and 3 on sensors 2 and 4, and *vice versa*, are eliminated. In a case of taking the data in a turbulent flow all four sensors have to be used and calibrated simultaneously.

The probe dimensions are: a = 0.41 mm and b = 0.61 mm giving the inclination angle α = 34°. A 90% platinum and 10% rhodium, 2.5 μm sensor wire is used.

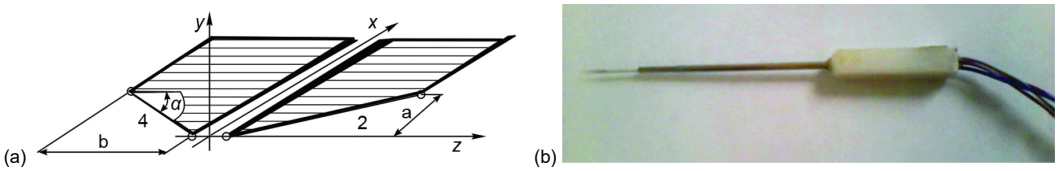

Figure 4. A sketch (a) and photo (b) of two sensor V-shaped probe

The probe is placed in a calibration apparatus shown in sketch of fig. 5. By variation of angle ξ and angle θ a 3-D flow field U, V, and W is induced:

$$U = V_R \cos\xi, \qquad V = V_R \sin\xi \sin\theta, \qquad W = V_R \sin\xi \cos\theta \tag{12}$$

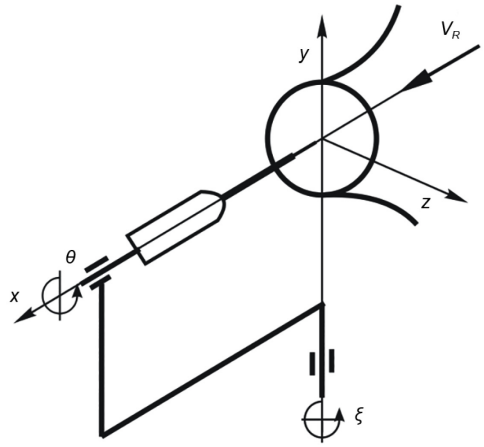

Figure 5. A schematic view of calibration apparatus

In the first two tests, angle ξ is varied in the range ±30° with step of 5° and angle θ in the range 0-360° with step of 45°. This way 76 calibration points, needed to determine the calibration coefficients, were obtained. For each value of angle θ, the variation of angle ξ was repeated with the probe rotated for 90° in order to get the response of sensors 1 and 3. In the same way we conducted the third test, but in this test angle ξ is varied in the range ±35° with step of 5°, giving 84 calibration points to determine new values of the calibration coefficients.

Probe is heated by a modified constant temperature anemometer circuits designed by AA Lab Systems with a frequency response of 50 kHz at 1.35 overheat ratio, what corresponds to approximate 290 °C sensor temperature. This way a reasonable sensitivity with minimal sensor thermal contamination is provided. The data were processed using a data translation four channel A/D converter with 100 kHz sampling rate. The probe was calibrated in a potential core of the free round jet of open laboratory wind

tunnel, producing a steady air nozzle flow in the range of 0-30 m/s with a negligible turbulence level.

Magnitude of velocity was maintained constant by electronically controlled fan rotation rate on 2027 rpm (5.877 m/s). The calibration procedure was conducted according to [9] when the algorithm based on King-Jorgensen, eq. (1) and eq. (2), is tested *i. e.* [1] when the algorithm based on *generalized hot-wire cooling law*, eq. (6) and (7) is tested. Calibration coefficients A_i, B_i, k_i, and h_i (in the case of King-Jorgensen test), and a_{ik}, b_{ik} (in the case of *generalized hot-wire cooling law*), were determined by least square fittings.

The comparison of measured values of the three velocity components obtained by *three against one* algorithm and nominal (induced) values for θ = 45° and various values of angle ξ, is given in fig. 6.

As it can be seen from fig. 6, the results of data processing by the *three against one* algorithm, for θ = 45°, and angle ξ in the range of –30° to +30°, in steps of 5°, based on *generalised cooling law* show much better agreement with induced (nominal) velocity then algorithm based on King-Jorgensen cooling law. This is particularly evident for the U velocity components and high values of ξ. One explanation for this should be sought in the fact that calibration coefficients in *generalised hot-wire cooling law*, include thermal contamination and geometrical imperfections lumped together. From the other side, in the presented *three against one* algorithm, based on King-Jorgensen cooling law, an averaged value of coefficients k_i and h_i (i = 1-4), for all tested angles θ and ξ, is used. It is known that the value of the coefficient k_i and h_i (i = 1-4) are varied with the direction of velocity vector as it is stated in [10]. This fact causes that discrepancy between the induced and calculated velocity components especially at the higher values of angle ξ, for which the biggest difference between averaged and real value of coefficient k_i and h_i (i = 1-4) is evident. Additional factor that could affect the accuracy of the results based on the equations of King and Jorgensen, eqs. (1), (2), and (4), is the value of the inclination sensor angles. An error in measuring of these angles is always present.

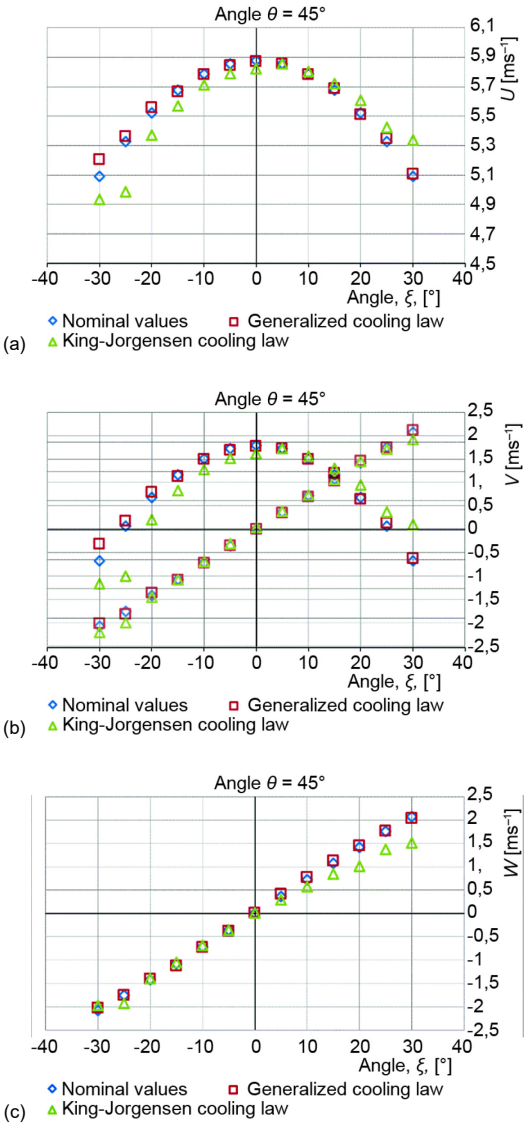

Figure 6. The comparison of measured and induced values of *U*, *V* and *W* components obtained by the *three against one* algorithm for θ = 45°; (a) *U*-component, (b) *V*-component, (c) *W*-component

Relative error in magnitude of velocity vector determined by calculated components *U, V,* and *W* by the *three against one* algorithm is shown in fig. 7. Relative error is calculated by the following equation:

$$\varepsilon = \frac{\left|V_R - V_{R\text{cal}}\right|}{V_R} \cdot 100\% \tag{13}$$

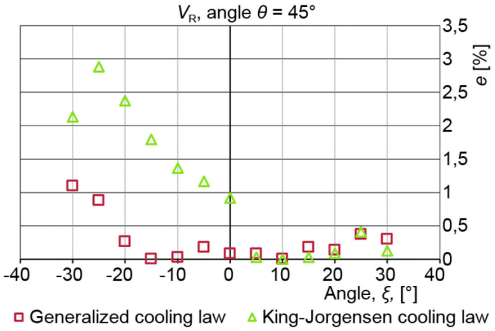

Figure 7. Relative errors in calculating magnitude of velocity vector, $\vec{V}_R$, by the *three against one* algorithm, for θ = 45°, based on two different cooling law

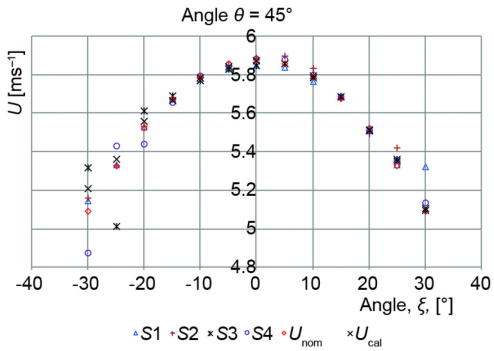

Figure 8. The solutions of four subsystem of eq. (9), for *U* velocity component (solutions are marked with *S1, S2, S3,* and *S4*), nominal, U_{nom}, and final solution, U_{cal}, obtained by the algorithm *three against one* based on *generalised cooling law*

where V_R is the magnitude of velocity vector (nominal velocity), and $V_{R\text{cal}}$ – the calculated magnitude by the *three against one* algorithm based on *generalized hot-wire cooling law* and King-Jorgensen cooling law.

Figure 8 shows all solutions of four subsystem of eq. (9), for U velocity component (solutions are marked with $S1$, $S2$, $S3$, and $S4$), nominal, U_{nom}, or induced value and final solution, U_{cal}, obtained by the *three against one* algorithm, based on *generalised cooling law* in the range of ξ ($-30° \leq \xi \leq 30°$) and $\theta = 45°$.

As it can be seen from fig. 8, for $\xi = -30°$, algorithm *three against one*, discards the worst of subsystems of eq. (9) (the subsystem $S4$, with relative error 4,45%), and from the rest three subsystems ($S1$, $S2$, and $S3$) calculates the final value U_{cal} (as the mean solution of the obtained values from subsystem $S1$, $S2$, and $S3$).

Final value U_{cal} (relative error 2.32%), can be in some cases obviously less accurate then a solution of some of the subsystems of eq. (9). For example, for $\xi = -30°$, solution of subsystems $S1$ and $S2$ are more accurate than the final solution. It is clear from fig. 2 that sensors 1 and 2 are the most aligned with the velocity vector. So, the subsystems containing these two sensors will give the highest measurements error. This is obvious from fig. 8. Similar situation is for $\xi = -25°$ and $\xi = -20°$. This means that a possibility of discarding more than one solution in some cases should be analysed too.

The final solutions calculated by the algorithm *three against one* are obviously between obtained ends solutions *i. e.* can not be the worst one of the four subsystem of eq. (9). As it can be seen from fig. 8, with increasing of angle ξ, in general case, the differences between the four subsystem solutions of eq. (9) are getting bigger too. This is due to the imperfections of the cooling law for higher values of angle ξ for which the velocity vector can get

more aligned with the axis of some of the three sensors in the subsystems of eq. (9). As a consequence some of the four subsystems will be more in error than the others.

Taking the maximal values of coefficients h_i and k_i ($h_4 = 1.5$, $k_4 = 0.165$), it follows from eq. (2) that the practical border of uniqueness range is $\xi_{cr} = 41.21°$ well above the maximal value of angle ξ. This means that all experimental measurements in this cases, are conducted inside the border of uniqueness domain and that the measurement errors are due to the imperfection of cooling laws only.

In the third test, the results obtained by the *three against one* algorithm for the U-velocity component are compared with the one of the best known approach described in [1], using real experimental data, for two ranges of angles ξ and $\theta = 45°$. Both methods were based on *generalised law of hot-wire cooling*. The results, in a case when angle ξ change its value from –30° to +30°, in steps of 5° is shown, fig. 9(a), and in a case when angle ξ change its value from –35° to +35°, in steps of 5° is shown, fig. 9(b).

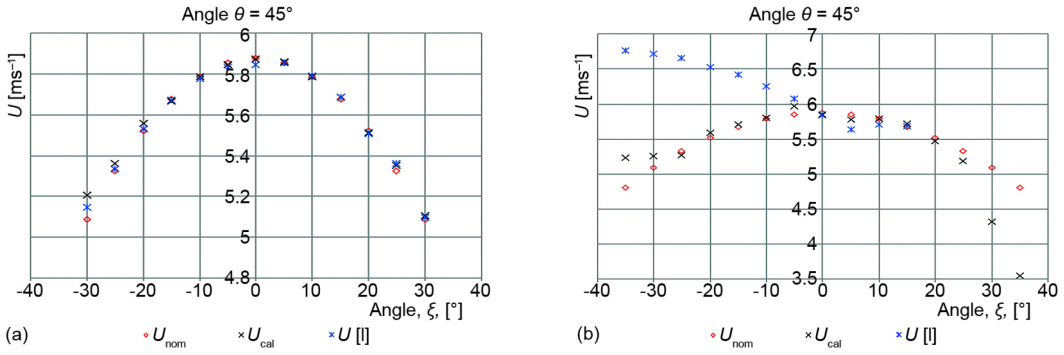

Figure 9. The comparison of U-velocity component U_{cal} (obtained by the *tree against one* algorithm), and U [1] (obtained by method presented in [1]), for $\theta = 45°$; (a) in the region of $-30° \le \xi \le 30°$, (b) in the region of $-35° \le \xi \le 35°$

As can be seen from fig. 9(a) ($-30° \le \xi \le 30°$) both methods have god accuracy in almost all measurement points. The results obtained by the method presented in [1] is slightly better for high negative ξ. That is not the case in the range of $-35° \le \xi \le 35°$, fig. 9(b), where in almost all measurement points (except for $\xi = 15°$), the *three against one* algorithm, U_{cal}, is more accurate. For $\xi \ge 20°$ the accuracy can not be compared because the method presented in [1] did not converge. Similar results are obtained for the V and W velocity components in the range of $-0° \le \theta \le 360°$.

It is clear that *three against one* algorithm is more accurate if the higher values of angle ξ are included. For the difference from the *three against one* algorithm, method presented in [1], U [1], uses only two of four possible sets of eq. (9), selecting only the more accurate one of two possible solutions.

The cooling law imperfection does not affect each set of eq. (9) to the same extent. The more is the velocity vector aligned to a sensor axis the higher will be the error due to the calibration procedure and *vice versa*. If the inclination angle of velocity vector toward the probe axis is small, each set of eq. (9) will give the results of similar accuracy. By increasing the velocity vector inclination angle some of the sets of sensors in eq. (9) will get more while the other will get less aligned with velocity vector. In other word the difference in accuracy of various sets of sensors will go up, one set will increase the accuracy while the other will de-

crease it. The more sets of eq. (9) we have available the higher is the probability to have one with the best accuracy. This is why the *three against one* algorithm is giving better results when the higher values of angle ξ are included. This algorithm discards the solution with the worse accuracy and take the mean values of the other three. In most cases, much better results will be achieved if the set with the best accuracy is selected only. It is clear from fig. 8 that in most cases, at least one such set always exist. A more complex algorithm providing this selection should be subject of further research.

Conclusions

In the region near the border of uniqueness domain, the *three against one* algorithm showed some advantage in comparison to the one of the best known method presented in [1]. For the difference from this method, the *three against one* algorithm always converges. In the most of the points where both methods converge, the *three against one* algorithm gives better accuracy. Still, this accuracy is not high enough. One of the possibilities to increase it is to improve the algorithm of the selection of the best sensor combination. Rather than discarding the worse one and taking the mean of the other three, the choice of the best one is more promising, what should be the subject of further research.

In addition, it is confirmed that algorithm based on *generalized hot-wire cooling law* gives much better results than algorithm based on King-Jorgensen cooling law, even inside the border of uniqueness domain. A more refined calibration procedure in comparison to the generalised cooling law is necessary around and beyond the border of uniqueness domain. If such a method is developed the advantage of the *three against one* algorithm in this region will come to the first place. It will enable the right choice of physical among rather high number of non unique solutions.

Acknowledgment

The authors thank Mr Petar Vukoslavčević, member of the Montenegrin Academy of Science and Arts and full professor at the Faculty of Mechanical Engineering, University of Montenegro, for providing measuring equipment and conditions at the laboratory of the Faculty of Mechanical Engineering in Podgorica, as well as for his assistance in preparing of this article.

Nomenclature

A – calibration coefficient in King's law, [V^2]
a_{ik} – hot-wire generalised cooling law coefficients, [–]
B – calibration coefficient in King's law, [V^2]
b_{ik} – hot-wire generalised cooling law coefficients, [–]
CTA – constant temperature anemometar
c_{ij} – generalised law of hot-wire cooling calibration coefficients, [–]
E – voltage drop on hot-wire probe, [V]
h – King-Jorgensen calibration coefficient for binormal velocity component, [–]
k – King-Jorgensen calibration coefficient for tangential velocity component, [–]
p – exponent in King's law, [–]
U – x component of fluid velocity, [ms^{-1}]
U_{cal} – calculated component of velocity U, [ms^{-1}]
U_{nom} – induced (nominal) component of velocity U, [ms^{-1}]
$U_{\mathrm{m}l}$ – mean value of solutions components of velocity U, in each step of iteration l, [ms^{-1}]
U_{rl} – solution for component of velocity U, from subsystem of equation r in each step of iteration l, [ms^{-1}]
V – y component of fluid velocity, [ms^{-1}]
V_{b} – binormal velocity component, [ms^{-1}]
V_{eff} – fluid effective cooling velocity, [ms^{-1}]
V_{effg} – generalised fluid effective cooling velocity, [ms^{-1}]
V_N – component of velocity vector perpendicular to the sensor longitudinal axis, [ms^{-1}]
V_{n} – velocity component normal to sensor, [ms^{-1}]
$V_{\mathrm{m}l}$ – mean value of solutions components of velocity V, in each step of iteration l, [ms^{-1}]

$\vec{V}_R$ – fluid velocity vector, [ms^{-1}]
$V_{R\text{cal }l}$ – calculated magnitude fluid velocity vector, [ms^{-1}]
V_{rl} – solution for component of velocity V, from subsystem of equation r in each step of iteration l, [ms^{-1}]
V_t – tangential velocity component, [ms^{-1}]
V_{vz} – spanwise velocity component, [ms^{-1}]
W – z component of fluid velocity [ms^{-1}]
W_{ml} – mean value of solutions components of velocity W, in each step of iteration l, [ms^{-1}]
W_{rl} – solution for component of velocity W, from subsystem of equation r in each step of iteration l, [ms^{-1}]

Greek symbols

α – hot-wire probe to prongs inclination angle, [°]
ε – relative error in magnitude of velocity vector, [%]
θ – fluid velocity directional angle around x-axis, [°]
ξ – fluid velocity directional angle around y-axis, [°]

References

[1] Vukoslavčević, V. P., Petrović, V. D., *Multiple Hot-Wire Probes*, Montenegrin Academy of Sciences and Arts, Podgorica, Montenegro, 2000
[2] Willmarth, W., Geometric Interpretation of the Possible Velocity Vectors Obtained with Multiple-Sensor Probes, *Physics of Fluids*, *28* (1985), 2, pp. 462-465
[3] Dobbeling, K., *et al.*, Basic Considerations Concerning the Construction and Usage of Multiple Hot-Wire Probes for Highly Turbulent Three-Dimensional Flows, *Measurement Science and Technology, 1* (1990), 9, pp. 924-933
[4] Vukoslavčević, V., *et al.*, An Analytical Approach to the Uniqueness Problem of Hot-Wire Probes to Measure Simultaneously Three Velocity Components, *Measurement Science and Technology, 15* (2004), 9, pp. 1848-1854
[5] Petrović, V. D., *et al.*, Enlarging the Uniqueness Cone of the Nine-Sensor, T-Configuration Probe to Measure the Velocity Vector and the Velocity Gradient Tensor, *Measurement Science and Technology, 21* (2010), 6, ID 065401
[6] Šajn, V., *et al.*, Algorithm for Velocity Vector Calculation for Constant Temperature Hot-Wire Anemometer, *Proceedings*, Kuhljevi dnevi, Cerklje na Gorenjskem, Slovenia, 2009, pp. 9-16
[7] Šajn, V. *et al.*, Mathematical Algorithm for Calculating the Velocity Vectors of Fluid by CTA in Spherical Coordinates, *Journal of Mechanics Engineering and Automation*, *2* (2012), 8, pp. 476-486
[8] Kotur, M., *et al.*, The Mathematical Algorithm for a Multi-Channel CTA Anemometer in Spherical Coordinates, *Proceedings,* 11th Int. Conference DEMI 2013, Banja Luka, Bosnia & Herzegovina, 2013, pp. 785-790
[9] Bruun, H. H., *et al.*, Calibration and Analysis of X Hot-Wire Probe Signals, *Measurement Science and Technology, 1* (1990), 8, pp. 782-785
[10] Chew, Y. T., Ha, S. M., The Directional Sensitivities of Crossed and Triple Hot-Wire Probes, *Journal of Physics E: Scientific Instruments, 21* (1988), 6, pp. 613-620

Paper submitted: June 30, 2017
Paper revised: November 25, 2017
Paper accepted: November 25, 2017